International Journal of Advance Research in Engineering, Science & Technology(IJAREST),
ISSN(O):2393-9877, ISSN(P): 2394-2444,
Volume 2,Issue 12, December- 2015, Impact Factor: 2.125

MODE-I TRACTION-SEPARATION LAW OF AN ADHESIVE JOINT

***Jay Mandaliar*[1], *Prof. R. B. Barjibhe*[2]**

[1] *Department of Mechanical Engineering, S.S.G.B.C.O.E.T, Bhusawal, jaymandalia@gmail.com*
[2] *Department of Mechanical Engineering, S.S.G.B.C.O.E.T, Bhusawal, rahulbarjibhe@yahoo.*

Abstract

Adhesive bonding is a viable alternative to traditional joining systems (e.g., riveting or welding) for a wide class of components belonging to electronic, automotive, and aerospace industries. However, adhesive joints often contain flaws; therefore, the development of such technology requires reliable knowledge of the corresponding fracture properties. This study deals with ideology to obtain a specific Traction-Separation Law based on the problem for PMMA/Epoxy adhesive joint along with crack-growth propagation and crack length relation establishment, on Mode-I conditions. This information is valuable for predicting the durability of a structure containing adhesively bonded joints.

Keywords-*adhesive joints, fracture, crack propagation, mode-I failure, Traction-Separation.*

I. INTRODUCTION

With the increasing demands from the customers and industry, it is required to stimulate new technology. For instance, in Automobile sector, the present scenario is increasing light weighted technology with maintaining the standards in emission and failure criterions. When it comes to joints, this light weighted combination is required to be joined with high strength low cost materials. These materials are known as adhesives, which, adds little wright to the structure and combination of joining even two dissimilar metals and non-metals is possible which is not possible even with welded joints. The use of adhesive joints in automotive, aerospace, biomedical, and microelectronics industries is widespread; however, inaccurate joint fabrication or inappropriate curing may cause the presence of bubbles, dust particles or un-bonded areas in the bond line. As a result of which it is mandatory to assess the reliability of this adhesive joints in events of fracture in order to avoid an accident. In recent years many members of the fracture community have adopted a cohesive zone model, based upon traction-separation relations, to simulate crack propagation. The two key parameters defining a Traction-Separation (T-U) relation are the work of separation (the area under the T-U curve) and the peak separation stress. The T-U approach appears particularly promising for several reasons.

II. LITERATURE SURVEY

Hutchinson and Suo, a practical approach for characterizing the adhesion of polymer coatings to metal substrates is to use sandwich specimens, which can be analyzed using interfacial linear elastic fracture mechanics (LEFM) concepts. ***Wang,*** however, there can be limitations to the use of LEFM in sandwich structures. The first is that the assumed stress fields are not rigorously correct, for example, in the case of large-scale plasticity or in the case of very thin layers where the K-dominant field cannot develop. ***Li et al.,*** the second is that some joints may not have macroscopic defects large enough to be considered cracks for the purpose of fracture mechanics. ***Dugdale and Barenblatt,*** these issues can compromise the utility of LEFM and alternative approaches must be sought. Cohesive zone modeling is one such approach. The key concept of cohesive zone modeling is that the failure process zone can be described by a traction–separation law; more specifically, the cohesive traction, σ(δ), can vary along the failure process zone, but only depends on the local opening, δ. The key is the introduction of a second fracture parameter, e.g., the cohesive strength, in addition to the fracture toughness. This cohesive strength relates the toughness to the critical crack-tip opening required for crack propagation. Recently cohesive zone modeling has been applied to solve interfacial fracture problems. ***Yang and Thouless,*** proposed a modified criterion for mixed-mode interfacial fracture, in which fracture occurs when the mode 1 and mode 2 energy release rates for the cohesive zone reach a critical value. Nevertheless, in both criteria, with independently characterized mode 1 and mode 2 traction–separation laws available, mixed-mode problems with a range of fracture mode-mixes can be fully solved. ***Swadener and Liechti*** examined cohesive zone modeling for a wide spectrum of interface problems, such as glass/epoxy interfacial fracture and adhesion. ***Massabo et al.,*** examined delamination in stitched composites considering the LEFM model in adhesive bonded joints. ***Shirani and Liechti*** found out plastic dissipation in thin debonding films during their experimental work over adhesive bonded joints. ***Mohammed and Liechti*** were the first to identify the crack nucleation at bi-material corners during the mode-1 and mixed mode conditions. ***Kinloch et al.; Kim and Aravas; Wei and Hutchinson; Yang et al.,*** experimentally found out that peeling apart from delamination occurs at the joints when adhesive bonded joints are subjected to various loadings.

Two methods that yield the traction–separation law directly from experiments without such comparison are available.

Cotterell and Mai; Pandya and Williams, one is through direct tension or shear experiments, however, in these experiments, the damage evolution across the width of the specimen must be uniform, which is usually difficult to achieve. ***Li et al.,*** in the second approach, the cohesive law is derived from simultaneous measurements of the J-integral and the end-opening (both normal and shear) of the cohesive zone. This has been successfully employed in the extraction of traction–separation laws for cementitious components. ***Sorensen***, successfully employed the same for adhesive bonds while, ***Sorensen and Jacobsen,*** employed the approach for fiber-reinforced composites.

III. CONCEPT OF CHESIVE ZONE

3.1 Cohesive Zone Model.

The cohesive element behavior is governed by a traction-separation law or cohesive law, relating element stress or traction to the opening (or nodal displacement). The constitutive behavior of cohesive elements is, in contrast to general finite element formulations with a continuous structural response, characterized by the relation between a crack tip opening value δ and the cohesive tractions T.

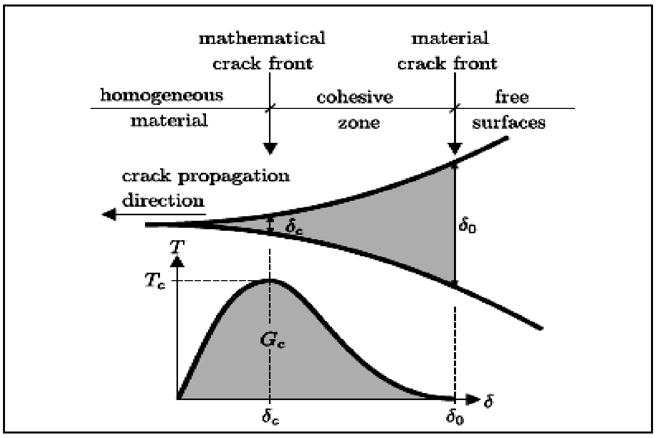

Figure 3.1: Cohesive Zone model and assumptions at the crack tip.

A large number of problem dependent and phenomenological or physically motivated traction separation laws (TSL) are proposed in the literature. Usually, the qualitative shape of these functions is similar. Starting at the traction free un-deformed state, the value of T increases with the separation of the crack surfaces up to a maximum value T_0 and decreases up to zero when complete separation occurs at a specific separation value δ_0. Mathematically a cohesive zone model is described by a cohesive law or the relationship between the cohesive traction σ and the opening displacement (separation) δ of the cohesive surfaces as follows:

$$\sigma = \sigma_c f(\delta/\delta_c) \quad (3.1)$$

where, σ_c is the peak cohesive traction, δc a characteristic opening, and f a dimensionless function describing the shape of the cohesive traction–separation curve (cohesive curve).

3.2 Traction Separation Law.

The form of the function T(δ) given in eq. (3.2) is defined in the TSL. Since the cohesive model is a phenomenological model there is no evidence which form to take for T(δ). So it has to be assumed independent from the material as a model quality. In the literature one can find several approaches.

$$\Gamma_0 = \int_0^{\delta_0} T(\delta)\,d\delta \quad (3.2)$$

Although a variety of geometry shapes have been used for this TSL (fig. 3.2), a bilinear form is commonly implemented for modeling.

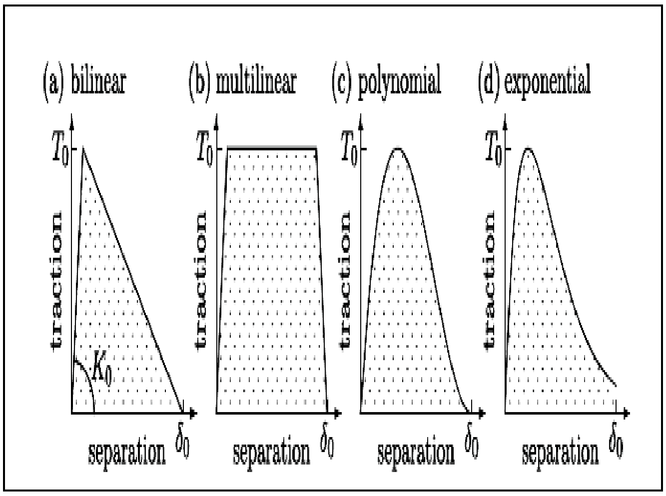

Figure 3.2: Basic Shapes Of Most Common TSL Formulations

IV. EXPERIMENTAL WORK

The double cantilever beam (DCB) configuration was used to determine the mode 1 traction–separation laws. [1] The specimen geometry and the loading are shown in Fig. 2(a). A pre-existing crack in the middle of the adhesive layer was cut using a sharp razor blade. It turned out that the fracture process zone in these experiments was large [25].Consequently, it was necessary to include [27] the contribution of the rotation near the crack front to the J-integral through,

$$J = 12\frac{(pa)^2}{Eh^3} + P(w_1' + w_2') \quad (5.1)$$

where P is the applied load per unit width, a is the crack length, h is the adherend thickness, and E is the elastic modulus of the steel adherends, and w0 1 and w02 are, respectively, the rotations of the upper and lower adherends at the crack tip.

The J-integral approach can be applied if the materials possess elastic stress–strain behaviour. The adherend is an elastomer, which was considered to be a nonlinear elastic material. Evaluating J-integral along a path just outside of the failure process zone yields

$$J = \int_0^{\delta'_n} \sigma(\delta_n)\,d\delta_n \quad (5.2)$$

where δ_n and δ'_n are the normal opening and the normal end-opening of the cohesive zone, respectively, and r is the normal traction. J reaches a steady-state value, J_{SS}, when δ'_n attains δ_{nc}, the critical normal end-opening. The entire failure process zone is described by the cohesive law.

Due to its path independence, the J-integral in Eq. (5.2) is equal to that obtained by Eq. (5.1). The normal end-opening δ'_n can be recorded in digital images, thus differentiation of Eq. (5.2) with respect to δ'_n gives,

$$\sigma(\delta'_n) = \frac{\partial J}{\partial \delta'_n} \qquad (5.3)$$

Thus, the mode 1 traction–separation law can be obtained by simultaneously measuring the J-integral and the normal end opening δ'_n.

For a Double Cantilever Beam geometry it is possible to find out the J Integral directly from experimental data under mode-I testing using the below mentioned relations.

$$J = \frac{12\, P^2 a^3}{E\, B^2 h^3} \qquad (5.4)$$

where, P is the load obtained directly during the experimental procedure, a is the crack length respective to the load, E is the Elastic modulus of the adhesive, B is the width of the adherents and h is the height of the adherent.

4.1 Specimen Preparation: [1]

The specimens were manufactured in two different ways.

- Method (1): The adherents were cut before the curing process, i.e. the specimens are put together individually during the curing process.
  The major problem with method (1) is to get parallel surfaces of adherends. With careful handling and a special fixture, this has been achieved to full satisfaction.
- Method (2): The two plates with applied adhesive are cured. After the curing process, specimens are cut from the plates.

The specimens for measuring the unconfined tensile behaviour of the PU bond were obtained from thin films. In this case, the PU fluid was applied on top of a PMMA block to form a thin film with thickness of 5 ± 0.1 mm.

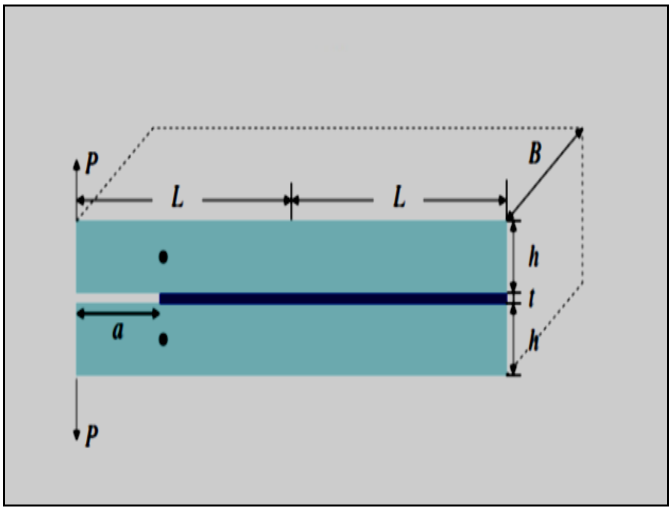

Figure 4.1: Schematics of the DCB test configuration and specimen (L = 45 mm, B = 20 mm, h = 10 mm and a = ranges from 05 to 25 mm) [1].

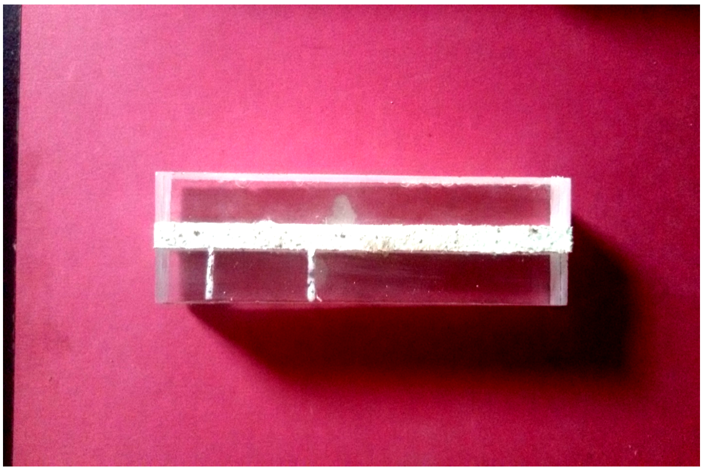

Figure 4.2: Actual DCB test configuration and specimen

Table 4.1 Dimension of Specimen Geometry

Sr. No.	Material	Length (mm)	Width (mm)	Height (mm)
1	PMMA	90	20	10
2	ADHESIVE	90	20	05

4.2 Testing of Specimen:

The most straightforward method to test adhesives was to use a test specimen made entirely of the adhesive material. When extracting constitutive relations from experiments on a thin film adhesive it is of utmost importance to know the stress distribution in the test specimen. As mentioned earlier, the stress distribution relies highly on the geometry of the specimen. The specimen as shown in fig 4.1 were prepared and tested on the universal testing machine. The required date was collected, such as maximum stress, maximum strain, the graph of load vs. displacement and the cohesive law has been derived from it.

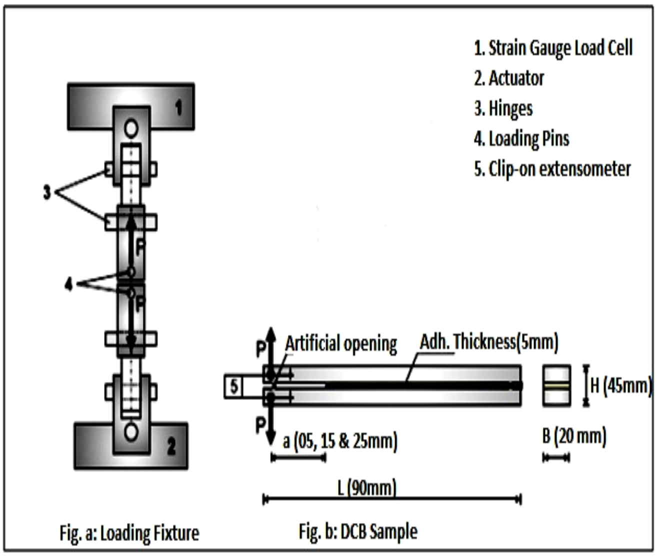

Figure 4.3: Schematic of fracture specimen and loading arrangement employed in the test[1].

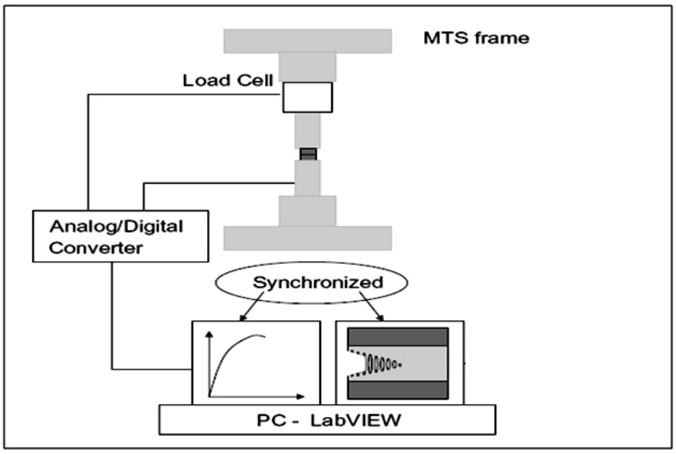

Figure 4.4: Schematic of experimental set-up [1]

All the experiments were conducted at room temperature using a load cell based materials testing system under constant crosshead speed. The material testing system used in the experimental work is a Universal Testing Machine with 10 KN Capacity and an accuracy of ± 1%. The differences noticeable under tensile loading and reliance on crosshead displacements would clearly lead to low measurements of moduli. In all total six experiments were conducted for the same samples with different openings as 2 samples of 05 mm opening, at the constant loading rate of 0.3 mm/s. [1]

V. RESULTS AND DISCUSSION

5.1 EXPERIMENTAL DATA SHEET OF SPECIMEN NO: 1,

Part	PMMA+ PU
Batch No.	DC Beam
Spec No.	No.1
Load Cell	9800N.
Temperature	25 °C
Speed	0.3 mm / sec
Pre Tension Load	0 N.
Gauge Length	100mm.
Peak Load	**331.24 N.**
Peak Elong	6.1 %
Break Load	90.16 N.
Break Elong	11.4 %
Tens Strength	3.312 MPa
CS Area	100.00 Sq.mm.
Width	5 mm
Thickness	20 mm
Break Strength	0.901MPa

With respect to the above experimental input data the next table shows the result values obtained from the experimental testing.

Table: 5.1 Experimental Result of Specimen 1.

Sr. No.	Time (sec)	CMOD Disp.(mm)	Load (N)	Crack Length(mm)
1	0.3	0.1	10.8	5
2	3.7	1	85.3	9.59
3	7.3	2	168.6	14.69
4	10.9	3	233.2	19.79
5	14.5	4	282.2	24.89
6	18.2	5	315.6	29.99
7	21.8	6	330.3	35.09
8	25.4	7	317.5	40.19
9	29	8	276.4	45.29
10	32.6	9	254.8	50.39
11	36.3	10	148	55.49
12	39.9	11	119.6	60.59
13	41.4	11.4	90.2	63.00

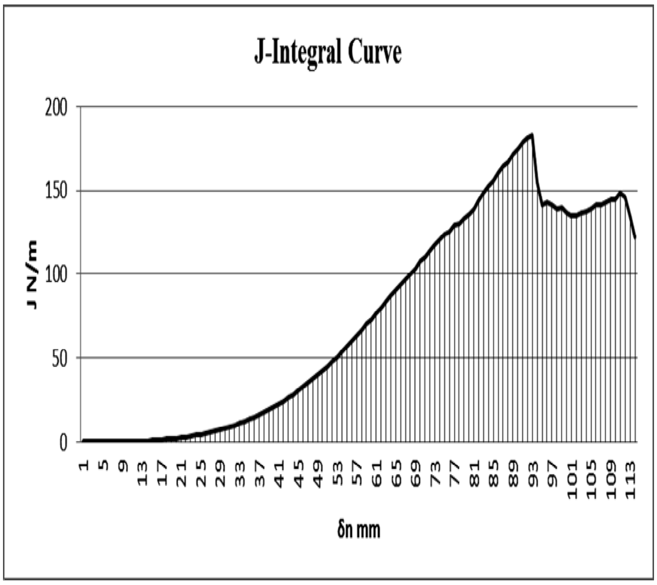

Figure 5.1: J-Integral for Specimen 1.

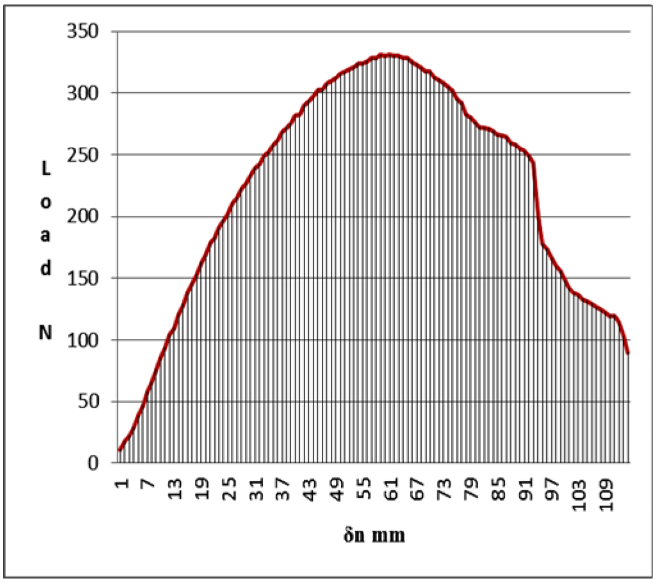

Figure 5.2: Load vs. Displacement of specimen 1.

International Journal of Advance Research in Engineering, Science & Technology(IJAREST), ISSN(O):2393-9877, ISSN(P): 2394-2444,
Volume 2,Issue 12, December- 2015, Impact Factor: 2.125

5.2 EXPERIMENTAL DATA SHEET OF SPECIMEN NO: 2

Part	: PMMA+ PU
Batch No.	: DC Beam
Spec No.	: No.2
Load Cell	: 9800N.
Temperature	: 25 ºC
Speed	: 0.3 mm / sec
Pre Tension Load	: 0 N.
Gauge Length	: 100mm.
Peak Load	: **234.22 N.**
Peak Elong	: 8.7 %
Break Load	: 29.40 N.
Break Elong	: 15.1 %
Tens Strength	: 2.342 MPa
CS Area	: 100.00 Sq.mm.
Width	: 5 mm
Thickness	: 20 mm
Break Strength	: 0.294 MPa

With respect to the above experimental input data the next table shows the result values obtained from the experimental testing.

Table 5.2: Experimental Data of the Specimen 2.

Sr. No.	Time (sec.)	Disp. (mm)	Load (N)	Crack Length (mm)
1	0.1	0	2	5
2	4.8	1.2	2	9.536
3	9.2	2.5	52.9	14.45
4	13.1	3.6	192.1	18.608
5	15	4.1	240.1	20.498
6	18.2	5	283.2	23.9
7	23.7	6.5	320.5	29.57
8	28	7.7	324.4	34.106
9	32	8.8	301.8	38.264
10	37.8	10.4	154.8	44.312
11	42.2	11.6	118.6	48.848
12	50.5	13.9	69.6	57.542
13	58	16	43.1	65.48
14	64.2	17.7	32.3	72

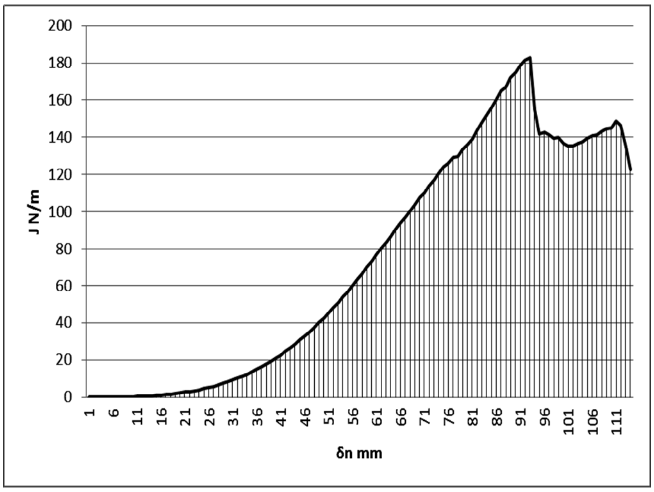

Figure 5.3: J-Integral for Specimen-2

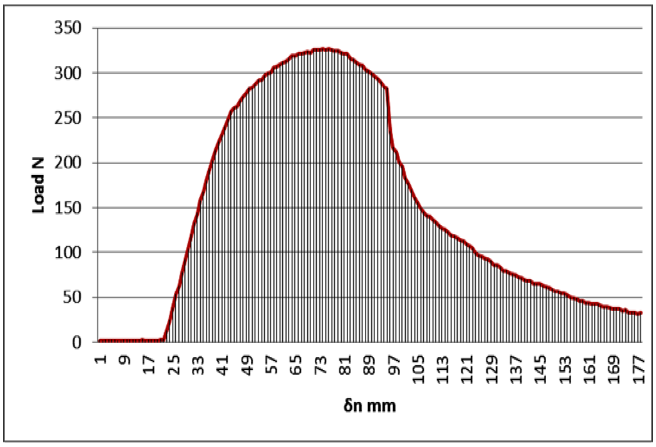

Figure 5.4: Load vs. Displacement of Specimen 2

VI. CONCLUSION AND FUTURE WORK

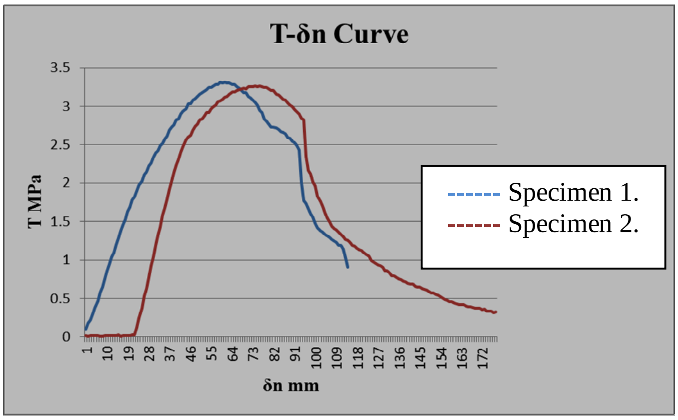

Traction-Separation relationship of specimen of an adhesive joint is the through which the load relationship for the particular set of combination can be easily evaluated. Here the results are evaluated for all the set combinations of tested under the tensile road. The graph 8.3 shows the comparison of traction-separation results of 5mm opening specimen under tensile load. The maximum load capacity for specimen no.1 was 332.21 N and the same for the specimen no. 2 was 326.34 N.

The maximum traction recorded was 3.32 MPa for specimen no. 1 and the same for the specimen no. 2 was 3.26 MPa. The maximum separation [CTOD] recorded for the specimen no. 1 was 11.4 mm and the same recorded for specimen no. 2 was 17.7 mm. the peculiarity of the Traction-Separation graph is the non-Zero opening recorded throughout the testing.

As such the work done is only for 5 mm opening, it can be concluded from the different specimen geometry with variable artificial crack length openings and the same law can be validated. It is clear from the observation of the results that the opening and the maximum load capacity for such a joint as compared with two separate geometries are same.

Apart from the work done emphasis can be laid upon the various parameters in future as mentioned below.

1. Fracture Tensile Tests were carried out at one opening only. However need to be conducted over a wide range of openings.
2. Fracture Tensile Tests were conducted for one strain rate only at room temperature. However it is needed to be conducted for different displacement rates.
3. The fracture toughness studies were done at room temperature. It is suggested to conduct the test at low temperatures and elevated temperatures.
4. The material geometry is needed to be tested for Mode-II (Shear Load) and Mode-III (Mixed Mode) loading.
5. Experimental evaluation can also be done with variable loading angles in order to study the various fracture parametric behavior.
6. Fatigue crack growth studies may also be conducted applying realistic spectrum variable amplitude conditions.
7. Strain field distribution may be obtained using soft computing and CAE software under various conditions.

VII. REFERENCES.

[1] Young Zhu, K. M. Liechti and K. Ravi-Chandar, "Direct extraction of rate dependent Traction-Separation for Polyurea/Steel Interface", 'International Journal of Solids and Structures', 2009, Vol. No. 46, PP 31-51.

[2] Adams, R.D., Comyn, J.C. and Wake, W.C. "Structural Adhesive Joints in Engineering", Chapman & Hall, London, 1997 UK.

[3]Akisanya, A.R., "Brittle fracture of adhesive joints", International Journal of Fracture, 1992, Vol. 58(2), PP 93–114.

[4] Barenblatt, G. I., "The Formation of Equilibrium Cracks during Brittle Fracture. General Ideas and Hypothesis, Axisymmetrical Cracks", 1959, PMM Journal of Applied Mathematics and Mechanics 23, 434–444.

[5]Barenblatt, G. I., "Mathematical Theory of Equilibrium Cracks", Advances in Applied Mechanics, 1962, Academic Press, New York, 55–125.

[6]Camacho, G. T., Ortiz, M., "Computational Modeling of Impact Damage in Brittle Materials", 1996, International Journal of Solids Structures 33, 2899–2938.

[7] Dugdale, D. S., "Yielding of Steel Sheets Containing Slits,'' 1960, Journal of Mechanics and Physics of Solids, Vol. 8, 100–104.

[8] Espinosa, H. D., Dwivedi, S., and Lu, H. C., "Modeling Impact Induced Delamination of Woven Fiber Reinforced Composites with Contact/Cohesive Laws", 2000, Computational Methods in Applied Mechanics, Vol. 183, 259–290.

[9] Espinosa, H. D., Zavattieri, P. D., Dwivedi, S., "A Finite Deformation Continuum/Discrete Model for Description of Fragmentation and Damage in Brittle Materials", 1998, Journal of Mechanics and Physics of Solids 46, 1909–1942.

[10] Foulk, J. W., Allen, D. H., Helms, K. L. E., "Formulation of a Three-dimensional Cohesive Zone Model for Application to a Finite Element Algorithm", 2000, Computational Methods in Applied Mechanics. Vol. 183, 51–66.

[11] Geubelle, P. H., and Baylor, J., "The Impact-Induced Delamination of Laminated Composites: A 2D Simulation", 1998, Composites, Part B, 29B, 589–602.

[12] Goglio, L., Rossetto, M., "Ultrasonic testing of anaerobic bonded joints". 2002, Ultrasonics, Vol. 40(1–8), 205–210.

[13] Jagota, A., P. Rahulkumar, Bennison, S. J., Saigal, S., "Cohesive Element Modeling of Viscoelastic Fracture: Application to Peel Testing of Polymers, 2000, International Journal of Solids Structures, Vol. 37, 1873–1897.

[14] Kinloch, A.J., "Adhesion and adhesives, Science and Technology. Chapman & Hall, London, 1986.

[15] Needleman, A., "An Analysis of Tensile Decohesion Along an Interface", 1990. Journal of Mechanics Physics of Solids, Vol. 38, 289–324.

[16] Needleman, A., "A Continuum Model for Void Nucleation by Inclusion Debonding". 1987. ASME Journal of Applied Mechanics, Vol. 54, 525–531.

[17] Siegmund, T., Brocks, W., "A Numerical Study on the Correlation between the Work of Separation and the Dissipation Rate in Ductile Fracture", 2000, Engineering Fracture Mechanics, 67, 139–154.

[18] Tvergaard, V., and Hutchinson, J.W., "The Relation between Crack Growth Resistance and Fracture Process Parameters in Elastic-Plastic Solids". 1992, Journal of Mechanics and Physics of Solids, Vol. 40, 1377-1393.

[19] Xu, X. P., and Needleman, A., "Numerical Simulation of Fast Crack Growth in Brittle Solids", Journal of Mechanics and Physics of Solids, 1994, Vol. 42, 1397–1434.

[20] Yang, B., "A Cohesive Zone Model for Fatigue Crack Growth in Quasibrittle Materials", 2001, International Journal of Solids Structures, 2001, Vol. 38, 3927–3944.

[21] M. Alfano, F. Furgiuele, L. Pagnotta, and G. H. Paulino, "Analysis of Fracture in Aluminum Joints Bonded with a Bi-Component Epoxy Adhesive", Journal of Testing and Evaluation, 2010, Vol. 39 No. 2, PP 1-8

[22] Parmigiani, J.P., Thouless, M.D., "The effects of cohesive strength and toughness on mixed-mode delamination of beam-like geometries", 2007, Engineering Fracture Mechanics Vol. 74, 2675–2699.

[23] Leffler, K., Alfredsson, K.S., Stigh, U., "Shear behaviour of adhesive layers". 2007, International Journal of Solids and Structures, Vol. 44, 530–545.